PRECLINICAL AND CLINICAL SPECTROSCOPY – Note

Magnetic Resonance in Medicine 80:36–41 (2018)

Sensitivity Enhancement for Detection of Hyperpolarized ^{13}C MRI Probes With ^{1}H Spin Coupling Introduced by Enzymatic Transformation In Vivo

Cornelius von Morze,[1]* James Tropp,[2] Albert P. Chen,[3] Irene Marco-Rius,[4] Mark Van Criekinge,[1] Timothy W. Skloss,[3] Daniele Mammoli,[1] John Kurhanewicz,[1] Daniel B. Vigneron,[1] Michael A. Ohliger,[1] and Matthew E. Merritt[5]

Purpose: Although ^{1}H spin coupling is generally avoided in probes for hyperpolarized (HP) ^{13}C MRI, enzymatic transformations of biological interest can introduce large ^{13}C-^{1}H couplings in vivo. The purpose of this study was to develop and investigate the application of ^{1}H decoupling for enhancing the sensitivity for detection of affected HP ^{13}C metabolic products.

Methods: A standalone ^{1}H decoupler system and custom concentric ^{13}C/^{1}H paddle coil setup were integrated with a clinical 3T MRI scanner for in vivo ^{13}C MR studies using HP [2-^{13}C]dihydroxyacetone, a novel sensor of hepatic energy status. Major ^{13}C-^{1}H coupling (1)$J_{CH} = \sim$150 Hz) is introduced after adenosine triphosphate–dependent enzymatic transformation of HP [2-^{13}C]dihydroxyacetone to [2-^{13}C]glycerol-3-phosphate in vivo. Application of WALTZ-16 ^{1}H decoupling for elimination of large ^{13}C-^{1}H couplings was first tested in thermally polarized glycerol phantoms and then for in vivo HP MR studies in three rats, scanned both with and without decoupling.

Results: As configured, ^{1}H-decoupled ^{13}C MR of thermally polarized glycerol and the HP metabolic product [2-^{13}C]glycerol-3-phosphate was achieved at forward power of approximately 15 W. High-quality 3-s dynamic in vivo HP ^{13}C MR scans were acquired with decoupling duty cycle of 5%. Application of ^{1}H decoupling resulted in sensitivity enhancement of 1.7-fold for detection of metabolic conversion of [2-^{13}C]dihydroxyacetone to HP [2-^{13}C]glycerol-3-phosphate in vivo.

Conclusions: Application of ^{1}H decoupling provides significant sensitivity enhancement for detection of HP ^{13}C metabolic products with large ^{1}H spin couplings, and is therefore expected to be useful for preclinical and potentially clinical HP ^{13}C MR studies. **Magn Reson Med 80:36–41, 2018. © 2017 International Society for Magnetic Resonance in Medicine.**

Key words: dihydroxyacetone; decoupling; dynamic nuclear polarization

INTRODUCTION

Routine hyperpolarization of ^{13}C-labeled small molecules using the process of dissolution dynamic nuclear polarization (1) has unlocked significant possibilities for clinical investigations of substrate-level metabolic activity in various disease states using ^{13}C MRI. Hyperpolarized (HP) [1-^{13}C]pyruvate (2) in particular has attracted considerable interest for applications to cancer and cardiovascular disease (3,4), with recent successful deployment into initial human studies (5,6).

^{1}H spin coupling is a major feature of ^{13}C NMR, yet has thus far played little role in the new field of HP ^{13}C MRI. In general, coupling to ^{1}H spins is conspicuously avoided in HP ^{13}C MRI in the effort to minimize loss of sensitivity caused by *J*-coupling and dipolar relaxation. Two initial studies found that ^{1}H decoupling can be moderately beneficial for HP [1-^{13}C]pyruvate MRI, by providing a modest degree of spectral narrowing of HP [1-^{13}C]lactate signal as a result of the elimination of long-range coupling to the distant methyl protons (7,8). Although there has been little further work in this area, other more recently introduced probes could benefit much more substantially from the application of ^{1}H decoupling. In particular, certain HP probes of interest with long T_1 relaxation times and minimal ^{1}H couplings are enzymatically transformed in vivo to important metabolic products with major ^{1}H couplings. This can occur with dehydrogenase activity at the labeled carbon site, exemplified by the reduction via lactate dehydrogenase of HP [2-^{13}C]pyruvate to [2-^{13}C]lactate (9), which is observed as a well-resolved ^{13}C signal doublet at 3 T ($J = 146$ Hz). Elimination of such large couplings, however, introduces high decoupling power requirements, which in turn require exceptionally good isolation between multinuclear RF channels, which is not typical for clinical MRI systems.

The new work presented here was inspired by the recent development of the new HP probe [2-^{13}C]dihydroxyacetone (DHA) (10). Hyperpolarized [2-^{13}C]DHA is rapidly taken up into cells and phosphorylated to the

[1]Department of Radiology and Biomedical Imaging, University of California, San Francisco, California, USA.

[2]Berkshire Magnetics, Berkeley, California, USA.

[3]GE Healthcare, Toronto, Ontario, Canada.

[4]University of Cambridge, United Kingdom.

[5]Department of Biochemistry, University of Florida, Gainesville, Florida, USA.

Grant sponsor: NIH; Grant number: K01DK099451, R01DK105346, P41EB013598, and P30DK026743.

*Correspondence to: Cornelius von Morze, Ph.D., Department of Radiology and Biomedical Imaging, University of California, San Francisco, 1700 Fourth Street, Byers Hall Suite 102, San Francisco, CA 94158, USA.
E-mail: cornelius.vonmorze@ucsf.edu

Received 6 August 2017; revised 28 September 2017; accepted 17 October 2017

DOI 10.1002/mrm.27000
Published online 28 November 2017 in Wiley Online Library (wileyonlinelibrary.com).

metabolic intermediate dihydroxyacetone phosphate in vivo, with subsequent reduction at the labeled site using glycerol-3-phosphate dehydrogenase to form [2-^{13}C]glycerol-3-phosphate (G3P) (Fig. 1), which is observed as a ^{13}C signal doublet ($J = 148$ Hz), among other metabolic fates. The adenosine triphosphate–dependent metabolic conversion of HP [2-^{13}C]DHA to [2-^{13}C]G3P is a promising new marker of liver energy status, and was recently shown to be markedly attenuated in rats challenged with an adenosine triphosphate–depleting fructose load (11). Derangement of normal hepatic energy metabolism underlies the progression of nonalcoholic fatty liver disease to nonalcoholic steatohepatitis (12), suggesting high potential for the use of HP [2-^{13}C]DHA in the clinical assessment of nonalcoholic fatty liver disease. Development of improved clinical markers of nonalcoholic fatty liver disease status is in fact an urgent unmet clinical need because of the high prevalence of this disease and the serious limitations of liver biopsy, including invasiveness, sampling error, and limited applicability as a repeat measure (13).

In this work we show for the first time that application of ^{1}H decoupling for ^{13}C MRI of HP [2-^{13}C]DHA provides greatly enhanced sensitivity for in vivo detection of the metabolic conversion of [2-^{13}C]DHA to [2-^{13}C]G3P, in experiments conducted in a clinical MRI scanner environment, in which ^{1}H decoupling is not commonly used (14). To our knowledge, this is the first reported in vivo decoupling of HP ^{13}C resonances with large C-H couplings ($^{1}J_{CH} = \sim 150$ Hz), and the first application showing a major sensitivity benefit of ^{1}H decoupling for HP ^{13}C MRI studies in vivo.

METHODS

Hyperpolarization

For each experiment, a 40-μL sample consisting of 9M [2-^{13}C]DHA (Sigma ISOTEC, Miamisburg, Ohio) in 2:1 water:DMSO (v/v), mixed with 22-mM OX63 and 1.0-mM Gd-DOTA, was polarized for a period of approximately 1 h in a commercial Hypersense polarizer (Oxford Instruments, Tubney Woods, United Kingdom) operating at 3.35 T and 1.3 K. Each sample was subsequently rapidly dissolved in 4.3-mL phosphate-buffered saline, to yield an 80-mM sample of HP [2-^{13}C]DHA, which was then rapidly transferred to the MRI system.

Radiofrequency Coil Configuration

The MRI experiments were conducted in a clinical 3T MRI scanner (GE Healthcare, Waukesha, Wisconsin). A custom ^{13}C/^{1}H curved paddle-shaped surface coil, depicted in Figure 2, was constructed for the purpose of these studies (Berkshire Magnetics, Berkeley, California). The coil consisted of a pair of concentric octagonal elements tuned to ^{1}H (outer) and ^{13}C (inner) frequencies. As a single paddle, the B_1 fields of both coil elements, and consequently their transmit and receive profiles, fall off with distance from the coil. However, the larger outer loop falls off more slowly than the smaller inner loop. The inner loop was therefore tuned for ^{13}C to provide high sensitivity in rat liver and constructed with sufficient size for sensitivity throughout the rat liver (with some weighting toward the proximal liver region),

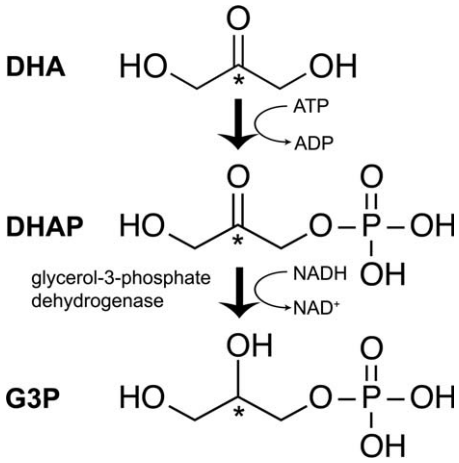

FIG. 1. Biochemical conversion of DHA to G3P in vivo. Position of the HP ^{13}C label is indicated by stars.

whereas the larger outer loop was tuned for ^{1}H to provide a relatively uniform decoupling field over this sensitive volume of the ^{13}C loop. The ^{13}C loop was equipped with passive ^{1}H blocking to prevent absorption of decoupling power. Although the ^{13}C loop was strictly operated in transceive mode, the ^{1}H loop was alternately used for imaging/spectroscopy (transceive mode) and ^{1}H decoupling (transmit only). Alternate RF coil setups were also tested, but none performed well at the required decoupling power levels, as a result of insufficient isolation between ^{1}H and ^{13}C channels.

^{1}H Decoupling

^{1}H decoupling power was provided by a commercial standalone rack-mounted assembly (GE Healthcare), with configuration similar to that described in a previous study (7), and depicted in Figure 3. A standalone device was used for this study, as neither of the clinical MRI systems sited near our polarizers support ^{1}H decoupling as a built-in feature. The assembly consists principally of a 2-kW, pulsed, 100-W, continuous-waveform radiofrequency (RF) amplifier (Herley, Lancaster, Pennsylvania), driven by a PC-controlled electronic signal generator (Agilent, Santa Clara, California). Output power was measured by feeding amplifier output through a 50-Ω dummy load with $|S_{21}|$ = approximately −30 dB and into an oscilloscope (Tektronix, Mukilteo, Washington). Crucially, the decoupling signal path is equipped with separate low- and high-power filters to block introduction of RF power at 32 MHz, which can easily obscure ^{13}C detection. Additionally, for this study, installation of a supplemental bandpass filter along the ^{13}C transmit-receive line (i.e., between ^{13}C loop and amplifiers) was required, to reduce receiver gain compression observed after activation of decoupling power approaching required levels. This filter was borrowed from a 3T small-animal MRI system (Bruker, Billerica, Massachusetts) sited nearby, and characterized by $|S_{21}(128\ \text{MHz})| = -58$ dB, $|S_{21}(32\ \text{MHz})| = -0.8$ dB.

Phantom Experiments

^{1}H decoupling for ^{13}C MRI was first tested in a thermally polarized glycerol phantom, consisting of a standard

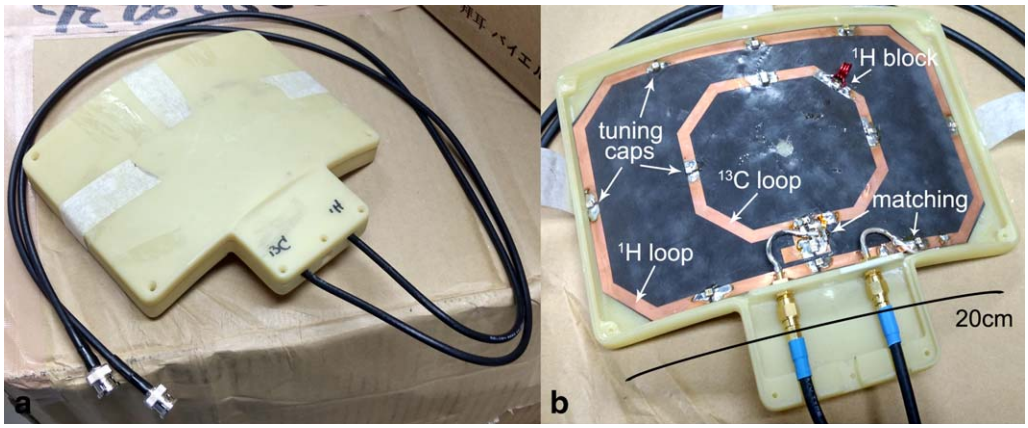

FIG. 2. Photographs of custom ^{13}C/^{1}H paddle coil used for ^{1}H-decoupled ^{13}C MRI experiments. **a**: Coil exterior and cabling. **b**: Coil internals consisting of concentric octagonal ^{1}H (inner) and ^{13}C (outer) elements, with key components labeled by arrows.

nitrile glove filled with 200-mL glycerol (natural abundance). Couplings observed in glycerol are very similar to the relevant case of [2-^{13}C]G3P. The glycerol phantom was placed on the described ^{13}C-^{1}H coil, along with two standard 100-mL 0.9% (wt/wt) saline intravenous bags to approximate rat-like loading. Nonselective pulse and acquire spectroscopy (pulse width = 500 μs, center frequency = 75 ppm, spectral points = 4096, sweep width = 25 kHz) was conducted with and without ^{1}H decoupling. A WALTZ-16 sequence (individual pulse width = 0.5 ms) was applied for ^{1}H decoupling (15), which was electronically triggered for activation during each readout interval using a scanner-derived transistor-transistor logic trigger signal. Outside of these intervals, decoupling power was attenuated by a factor of 49 dB using the decoupler's bilevel irradiation feature. The WALTZ-16 scheme was chosen because its bandwidth and insensitivity to B_1 inhomogeneity compare favorably with other possible schemes (15,16), and for the practical reason that it was already implemented on the standalone electronic signal generator.

Hyperpolarized ^{13}C MRI Experiments

Three rats each underwent back-to-back HP [2-^{13}C]DHA scans, with and without ^{1}H decoupling. All animal studies were conducted in accordance with a protocol approved by the University of California, San Francisco, Institutional Animal Care and Use Committee. Each rat was anesthetized using 1.5% inhalational isofluorane before having a tail vein catheter implanted and being positioned prone onto the coil with liver region directly above the ^{13}C loop. A heated water pad was placed under the rat to maintain body temperature. The first HP injection and scan applied ^{1}H decoupling, whereas the second injection and scan (approximately 90 min later, within the same scanning session) did not. A previous study applying similar methods showed that the extent of conversion of HP [2-^{13}C]DHA to HP [2-^{13}C]G3P in liver and kidney returns to a similar level within 80 min after the first injection (11). For in vivo experiments, effectiveness of decoupling was verified just before the HP experiment based on signal from a vial phantom containing 1-mL [2-^{13}C]glycerol (Cambridge Isotopes, Tewksbury, Massachusetts) placed adjacent to the rat. This vial was removed for each HP experiment. Each injection consisted of 2.2 mL of 80-mM HP [2-^{13}C]DHA delivered over 12 s, with dynamic nonlocalized spectroscopy as conducted in the phantom experiments (pulse width = 500 μs, center frequency = 75 ppm, nominal flip angle = 20°, spectral points = 4096, sweep width = 25 kHz). Excitation was

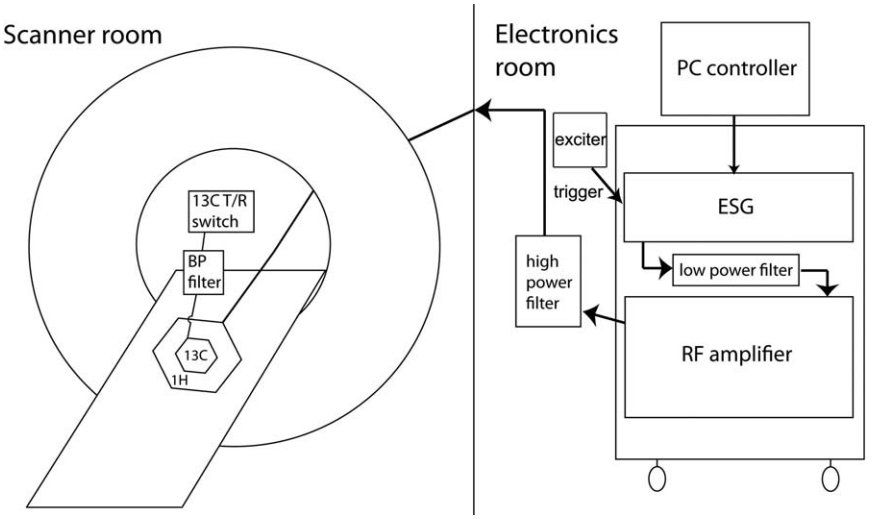

FIG. 3. Simplified schematic depiction of standalone accessory ^{1}H decoupler operation in conjunction with clinical 3T scanner used for HP ^{13}C MRI. Major components include (in electronics room adjacent to scanner): PC controller, electronic signal generator (ESG), transistor-transistor logic (TTL) trigger signal from system exciter board, 2-kW peak RF amplifier, and low- and high-power filters; and in scanner room: concentric ^{1}H (outer) and ^{13}C (inner, with passive ^{1}H blocking) coil elements, bandpass (BP) filter on ^{13}C channel installed between ^{13}C coil and ^{13}C transmit-receive (T/R) switch.

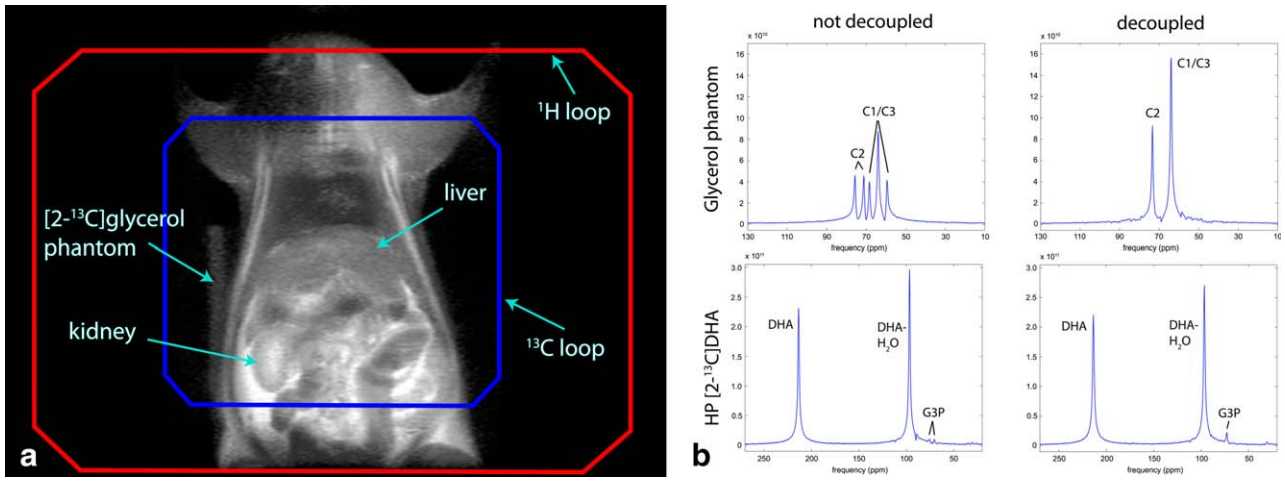

FIG. 4. Multinuclear RF coil setup for in vivo ^{1}H-decoupled HP [2-^{13}C]DHA scans in rats (**a**) and comparison of results with and without ^{1}H decoupling (**b**). **a**: Octagonal ^{1}H (outer) and ^{13}C (inner) coil traces are shown overlaid on a standard coronal anatomic localizer image acquired using the paddle's ^{1}H channel. **b**: ^{13}C MR spectra (magnitude) acquired in the clinical 3T MRI scanner with (right column) and without (left column) ^{1}H decoupling. Top row: Comparison of thermally polarized, nonenriched glycerol phantom spectra. Bottom row: Summed dynamic spectra from a pair of back-to-back HP [2-^{13}C]DHA experiments in one rat.

repeated dynamically every 3 s over 30 s, starting 20 s after the start of injection. Decoupling power was again attenuated by 49 dB between readout intervals, so the duty cycle for application of ^{1}H decoupling power was 5%.

RESULTS

As configured, optimal ^{1}H decoupling of thermally polarized ^{13}C spectra in the glycerol phantom was achieved at a measured decoupler output power of approximately 15 W (Fig. 4B, top row). The measured ^{13}C signal enhancements for both doublet and triplet resonances were close to the two-fold increases predicted from theory—2.0x in the case of the C_2 doublet, and 1.8x in the case of the C_1/C_3 triplet. There was no significant nuclear Overhauser effect enhancement, as the bilevel irradiation attenuation factor was set to a very large value of 49 dB.

Application of ^{1}H decoupling in the HP [2-^{13}C]DHA experiments collapsed the [2-^{13}C]G3P signal doublet into a singlet and greatly enhanced the sensitivity for detection of G3P (Fig. 4b, bottom row). The placement of the RF coil is shown in Figure 4a. Across the three rats, the summed [2-^{13}C]G3P peak signal was enhanced by an average factor of 71+/−29% ($P = 0.049$, paired two-tailed t-test). Dynamic HP [2-^{13}C]DHA spectra from one of the three rats scanned are shown in Figure 5, including data acquired with and without ^{1}H decoupling. In the absence of decoupling, the G3P doublet falls into the noise floor at an earlier time.

Occasional decoupling signal breakthrough was clearly detected in some ^{13}C transients, but effects were mild until especially high power levels exceeding our requirements, and thus did not generally interfere with ^{1}H-decoupled ^{13}C MR detection. Use of the supplemental bandpass filter along the transmit-receive line greatly reduced severe gain compression effects on the ^{13}C receiver, but resulted in an approximate 1-dB increase in transmit gain required to achieved a given flip angle, corresponding well to the measured filter insertion loss

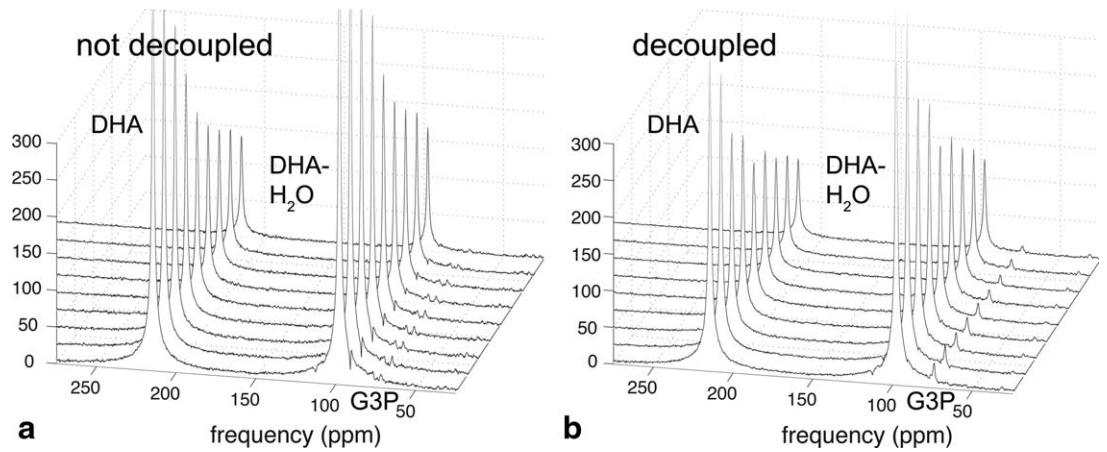

FIG. 5. Dynamics of HP [2-^{13}C]DHA spectra in one rat, for the cases of no ^{1}H decoupling (**a**) and ^{1}H-decoupled (**b**). The temporal dynamic spacing was 3 s, starting 20 s after the start of injection of HP [2-^{13}C]DHA. Magnitude NMR data are shown, scaled to approximate signal-to-noise ratio level.

$|S_{21}(32\ \text{MHz})| = -0.8$ dB, and establishing a relatively small upper bound on possible signal-to-noise ratio penalty associated with filtering.

DISCUSSION

Our results show the clear feasibility of ^{1}H decoupling of HP ^{13}C resonances with large *J*-couplings ($^{1}J_{CH} = \sim 150$ Hz) such as found in [2-^{13}C]G3P. This was accomplished using a standalone ^{1}H decoupler system integrated within a clinical MRI scanner environment, in which ^{13}C MR (let alone ^{1}H decoupling) is not commonly used. Customization of scanner hardware, including specialized RF coil design and use of supplemental filtering, was necessary to facilitate ^{1}H-decoupled ^{13}C MR at the required power levels.

Application of ^{1}H decoupling clearly resulted in a major sensitivity boost for detection of the HP metabolic product [2-^{13}C]G3P. This result exemplifies a new approach for enhanced detection of HP ^{13}C metabolic products, applicable for cases in which a long-lived HP precursor without significant ^{1}H coupling (e.g., [2-^{13}C]DHA) is transformed enzymatically in vivo into a HP metabolic product with major ^{1}H coupling (e.g., [2-^{13}C]G3P).

Excessive power deposition (i.e., specific absorption rate (SAR)) has practically limited the applicability of broadband ^{1}H decoupling schemes for ^{13}C MRS studies of humans (14). The SAR is a complicated function of RF coil and subject size, shape, and electrical properties, as well as RF pulse frequency, amplitude, and duty cycle (17). The massive sensitivity enhancement afforded by hyperpolarization could greatly reduce the cumulative power deposition required for acquisition of high-quality broadband decoupled ^{13}C MR spectra. With traditional thermally polarized ^{13}C experiments, the nuclear Overhauser effect enhancement associated with constant broadband decoupling generates up to three-fold signal-to-noise ratio gain for protonated carbons. Because the HP sample has a polarization far in excess of that produced by the nuclear Overhauser effect, our experiments were run in a gated decoupling mode (decoupling only during signal acquisition, or 5% duty cycle), significantly decreasing the SAR. The lowered SAR values should enable the application of these decoupling schemes in full field-of-view ^{13}C MR studies in humans.

Although precise SAR calculations or measurements are difficult, relatively simple calculations illustrate important considerations regarding the potential for clinical translation of these methods. Under simplifying quasi-static assumptions, the total instantaneous power deposition in a homogenous sphere irradiated by a uniform, linearly polarized RF magnetic field is given by $P_i = (\pi/15)(D/2)^5 \sigma \omega^2 B^2$, where D is the sphere diameter, σ is its RF conductivity, ω is the frequency of the RF field, and B is the RF field amplitude (18). For this study, we can infer that $B \approx 23\,\mu$T from the 90° pulse duration of 0.5 ms. Then, assuming that $\sigma = 0.4$ s/m in a spherical sample with $D = 8$ cm (i.e., loosely approximating a 300-g rat, similar to those used in this study), we can estimate that $P_i \approx 3$ W. In comparison to the measured amplifier output power of 15 W required to drive the surface coil used in this study, this is not an unreasonable estimate after accounting for cable losses and reflected power, as well as the relatively large coil size. Most importantly, the power equation shows that P_i scales sharply with sample diameter. For a 25-cm human abdomen, the calculated P_i required is predicted to rise to approximately 900 W. However, the *average* power is lowered by a factor of 20 by the low 5% duty cycle required in the described HP acquisition, leading to a more reasonable value of approximately 45 W. Moreover, the short total scan time of HP studies also leads to low cumulative RF exposure. If, however, we assume a worst-case scenario that all 15 W supplied by the amplifier is deposited into the subject, the expected power requirement for abdominal scanning scales to potentially excessive power levels, whereas head scanning (e.g., $D = 17$ cm) could still be reasonable, even though the amplifier used in this study is limited to 50-W output as configured. For optimal efficiency, use of a circularly polarized decoupling field would be highly desirable, as this would be twice as efficient per unit SAR (19). A further consideration is that dielectric effects are also more important in larger human-sized samples, requiring more sophisticated SAR analysis (20). In summary, fully establishing the feasibility of these ^{1}H decoupling methods in humans will depend on more detailed SAR analysis, and careful SAR monitoring will be required for translation into human studies.

Given that the metabolic conversion from HP [2-^{13}C]DHA to [2-^{13}C]G3P in vivo is a promising new marker of hepatic energy status, which is relevant to studies of nonalcoholic fatty liver disease, ^{1}H-decoupled HP ^{13}C MRI is of great interest for preclinical and potentially clinical studies of liver disease. Furthermore, the described development of an integrated system for simultaneous dual stimulation of ^{13}C and ^{1}H nuclei in a clinical scanner environment could also facilitate in vivo application of other advanced NMR methods potentially useful for HP ^{13}C MRI, such as ^{13}C-^{1}H polarization transfer (21).

REFERENCES

1. Ardenkjaer-Larsen JH, Fridlund B, Gram A, Hansson G, Hansson L, Lerche MH, Servin R, Thaning M, Golman K. Increase in signal-to-noise ratio of > 10,000 times in liquid-state NMR. Proc Natl Acad Sci USA 2003;100:10158–10163.
2. Golman K, in 't Zandt R, Thaning M. Real-time metabolic imaging. Proc Natl Acad Sci USA 2006;103:11270–11275.
3. Kurhanewicz J, Vigneron DB, Brindle K, et al. Analysis of cancer metabolism by imaging hyperpolarized nuclei: prospects for translation to clinical research. Neoplasia 2011;13:81–97.
4. Malloy CR, Merritt ME, Dean Sherry A. Could 13C MRI assist clinical decision-making for patients with heart disease?. Rizi R, editor. NMR Biomed 2011;24:973–979.
5. Nelson SJ, Kurhanewicz J, Vigneron DB, et al. Metabolic imaging of patients with prostate cancer using hyperpolarized [1-C-13]pyruvate. Sci Transl Med 2013;5:198ra108.
6. Cunningham CH, Lau JY, Chen AP, Geraghty BJ, Perks WJ, Roifman I, Wright GA, Connelly KA. Hyperpolarized 13C metabolic MRI of the human heart: initial experience. Circ Res 2016;119:1177–1182.
7. Chen AP, Tropp J, Hurd RE, Van Criekinge M, Carvajal LG, Xu D, Kurhanewicz J, Vigneron DB. In vivo hyperpolarized 13C MR spectroscopic imaging with 1H decoupling. J. Magn Reson 2009;197:100–106.
8. Marjańska M, Iltis I, Shestov AA, Deelchand DK, Nelson C, Uğurbil K, Henry P-G. In vivo 13C spectroscopy in the rat brain using hyperpolarized [1-(13)C]pyruvate and [2-(13)C]pyruvate. J Magn Reson 2010;206:210–218.

9. Hu S, Yoshihara HAI, Bok R, Zhou J, Zhu M, Kurhanewicz J, Vigneron DB. Use of hyperpolarized [1-13C]pyruvate and [2-13C]pyruvate to probe the effects of the anticancer agent dichloroacetate on mitochondrial metabolism in vivo in the normal rat. Magn Reson Imaging 2012;30:1367–1372.
10. Moreno KX, Satapati S, DeBerardinis RJ, Burgess SC, Malloy CR, Merritt ME. Real-time detection of hepatic gluconeogenic and glycogenolytic states using hyperpolarized [2-13C]dihydroxyacetone. J Biol Chem 2014;289:35859–35867.
11. Marco-Rius I, vonMorze C, Sriram R, et al. Monitoring acute metabolic changes in the liver and kidneys induced by fructose and glucose using hyperpolarized [2-13C]dihydroxyacetone. Magn Reson Med 2017;77:65–73.
12. Sunny NE, Bril F, Cusi K. Mitochondrial adaptation in nonalcoholic fatty liver disease: novel mechanisms and treatment strategies. Trends Endocrinol. Metab 2017;28:250–260.
13. Fitzpatrick E, Dhawan A. Noninvasive biomarkers in non-alcoholic fatty liver disease: current status and a glimpse of the future. World J Gastroenterol 2014;20:10851–10863.
14. de Graaf RA, Rothman DL, Behar KL. State of the art direct C-13 and indirect H-1-[C-13] NMR spectroscopy in vivo. A practical guide. Rizi R, editor. NMR Biomed 2011;24:958–972.
15. Shaka AJ, Keeler J, Frenkiel T, Freeman R. An improved sequence for broadband decoupling: WALTZ-16. J Magn Reson (1969) 1983;52:335–338.
16. de Graaf RA. Theoretical and experimental evaluation of broadband decoupling techniques for in vivo nuclear magnetic resonance spectroscopy. Magn Reson Med 2005;53:1297–1306.
17. Bottomley PA, ROEMER PB. Homogeneous tissue model estimates of RF power deposition in human NMR studies. Ann NY Acad Sci 1992;649:144–159.
18. Collins CM, Wang Z. Calculation of radiofrequency electromagnetic fields and their effects in MRI of human subjects. Magn Reson Med 2011;65:1470–1482.
19. Glover GH, Hayes CE, Pelc NJ, Edelstein WA, Mueller OM, Hart HR, Hardy CJ, O'Donnell M, Barber WD. Comparison of linear and circular polarization for magnetic resonance imaging. J Magn Reson (1969) 1985;64:255–270.
20. Tropp J. Image brightening in samples of high dielectric constant. J Magn Reson 2004;167:12–24.
21. Wang J, Kreis F, Wright AJ, Hesketh RL, Levitt MH, Brindle KM. Dynamic (1) H imaging of hyperpolarized [1-(13) C]lactate in vivo using a reverse INEPT experiment. Magn Reson Med 2018;79:741–747.